Available online at www.sciencedirect.com

ScienceDirect

Energy Procedia 45 (2014) 997 – 1006

Energy Procedia

68th Conference of the Italian Thermal Machines Engineering Association, ATI2013

Tumble motion generation in small gasoline engines: a new methodological approach for the analysis of the influence of the intake duct geometrical parameters

Federico Brusiani[a], Stefania Falfari[a,]*, Giulio Cazzoli[a]

[a]*Department DIN, University of Bologna, Bologna, 40136, Italy*

Abstract

For motorbike and motor scooter applications, the optimization of the tumble generation is considered an effective way to improve the combustion system efficiency and to lower the emissions, considering also that the two-wheels layout represents an obstacle in adopting the advanced post-treatment concepts designed for the automotive applications.
During the last years the deep re-examination of the engine design for lowering the engine emissions involved the two-wheel vehicles too. The IC-engine overall efficiency plays a fundamental role in determining the final raw emissions. From this point of view, the optimization of the in-cylinder flow organization is mandatory. In detail, in SI-engines the generation of a coherent tumble vortex having dimensions comparable to the engine stroke could be of primary importance to extend the engines' ignition limits toward the field of the dilute/lean mixtures.
The aim of the paper is to introduce a new analysis approach for a deep insight of the 3D-CFD results performed to assess the intake duct geometry influence on the tumble motion generation during both the intake and the compression strokes. All the CFD simulations presented in the paper were performed by the AVL-FIRE v.2010 CFD code on a SI 4 valve engine characterized by an unit displacement of 250 cm^3. The tumble structure was changed during the analysis by changing the angle set defining the intake port shape. The stroke-to-bore engine ratio was kept constant to 0.7. The effects of the tumble variations were evaluated in terms of the tumble ratio, the turbulent kinetic energy and the vortex characterization at IVC.

Keywords: Small Gasoline Engine; Tumble Motion; Tumble Torque; Turbulent Intensity; pdf distribution;

* Corresponding author. Tel.: +39-051-209.3316; fax: +39-051-209.3313.
E-mail address: stefania.falfari@unibo.it

doi:10.1016/j.egypro.2014.01.105

1. Introduction

Faster combustion and lower cycle-to-cycle variability are the two mandatory tasks in the naturally aspirated engines for lowering the emission levels and for increasing the efficiency. They allow to operate the engine with a high compression ratio and a small spark advance for the maximum brake torque reducing the fuel consumption. In order to speed up the combustion in the small engines the most effective ways are to promote the tumble flow at the end of the intake phase and the squish motion around TDC [1-4]. In particular in some previous papers [1, 5] the authors demonstrated the squish motion ineffectiveness in promoting the turbulence in the small bore engines. So in the present paper only the tumble flow is considered: it is maximized by optimizing the intake duct layout.

2. Literature summary on the tumble motion

The literature review collects different experience and evidence on the formation the tumble flows [6-10]. In [1] the authors carried out an analysis of a small 3-valves PFI engine characterized by a small bore and a high stroke-to-bore ratio. They compared three geometries differing only in the squish area distribution and values. In [2] the authors varied some engine parameters (the intake duct angle, the intake valve lift, the piston shape, and the compression ratio) for extracting a 'value scale' based on their influence on the tumble motion. Authors in [3] focused on the effect of the joint use of the tumble and the squish flows in promoting the in-cylinder turbulence for fast combustion purposes. The squish velocity to the tumble velocity ratio at TDC was used to evaluate the effectiveness of the joint use of the tumble and the squish flow. In [4] authors used the numerical simulation to assess the influence of some intake duct geometrical parameters on the tumble motion generation during both the intake and the compression strokes to highlight the turbulence production process. In [5] the authors presented a theoretical model capable of describing the interaction between the squish velocity and the tumble velocity depending on the engine class.

3. Paper framework

The aim of the paper is to introduce a methodology of analysis for the CFD simulation results presented in [4]: the numerical simulations were performed to assess the influence of the intake duct characteristic angles, visible in Fig. 1, for a certain engine class (C/D) on the tumble motion generation during both the intake and the compression strokes, and the turbulence production process. In Table 1, the main parameters characterizing the engine in analysis are summarized: the exhaust valve phase was not reported because the exhaust process was not considered. In detail, the present analysis concerns a systematic and parametric study of two intake duct parameters for a fixed engine class (constant C/D ratio). The present analysis is part of a more complex project involving the study of the effect on the tumble motion of the intake port parameters for engines having different C/D ratios and operating at partial load too.

The intake duct parameters analysed are the intake port angle, called α, and the intake manifold angle β defining the flow direction approaching the valve (Fig. 1). In the common practice the tumble motion analysis is carried out by means the tumble motion parameter and the mean turbulent intensity distribution in the whole combustion chamber and close to the spark plug location. Moreover a graphical analysis of the velocity flow field by means a plane cut is usually done for a deeper comprehension of the tumble motion formation. In the present paper a more accurate investigation of the flow field in the combustion chamber is presented: it is aimed to analytically determine the flow field organization and the turbulence distribution at the combustion start time. So the tumble torque and the vortex analysis at IVC were introduced in this technical dissertation. In particular the effect of the angles α and β on the intake flux fluidynamic was investigated splitting the intake curtain area into four main sections, as discussed in the paragraph below: the tumble torque parameter was introduced for the comparison. The aim was to give a deep insight of the effect of the intake port variation on the incoming flux and then on the tumble motion. Last of all for a proper comparison among the mean turbulent intensity distributions obtained with the four different intake duct configurations and for determining the best set-up finalized to have a proper level of turbulence close to the spark plug, the probability distribution function (pdf) at the ignition timing was derived.

In the present paper first of all the results carried out at an engine speed of 6500 rpm for the configurations listed in Table 2 are presented. These configurations came from a Full Factorial two levels approach. The minimum and the maximum value for each angle was set in order to preserve the head shape, which plays an important role in the tumble structure formation. The methodological approach adopted based on the CFD simulations was tested in the last years by the research group the authors belong to [11-15]. Details on the CFD simulation set-up could be find in [4].

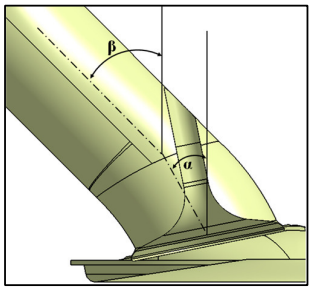

Fig. 1. Intake port parameter sketch. Modifying the α and β angles the intake port geometry was changed.

Table 1. Engine data.

Bore [mm]	102.0
Stroke [mm]	68.0
Conrod length [mm]	122.5
C/D	0.7
Compression ratio (RC)	11.0
Valve number	4.0
% squish area	10.8
Squish height at TDC [mm]	1.1
Inlet Valve Open	330° BTDC
Inlet Valve Close	610° BTDC

Table 2. Intake port parameters variation.

Case Number	α [°]	β [°]
1	37	45
2	37	55
3	47	45
4	47	55

4. CFD simulation results - Analysis

In this paragraph the results from the 3D CFD simulations were processed. As above discussed the results obtained along the intake/compression engine phases are separately presented in terms of:

1. The tumble ratio. The tumble ratio is the ratio between the instantaneous solid body equivalent angular velocity ω and the engine angular velocity. The angular velocity ω is the angular velocity of a rotating solid body of angular momentum equal to that of the instantaneous in-cylinder mass, evaluated with respect to an axis perpendicular to the cylinder axis and centered between the head and the instantaneous piston position.

2. The mean turbulent intensity, defined as the ratio between the turbulent fluctuating energy u' and the mean piston speed V_p. The turbulent fluctuating energy is a function of the turbulent kinetic energy k. In particular for the four different cases the probability distribution function of the mean turbulent intensity in a sphere centered around the spark plug and having a radius R of 1 cm was extracted. Then supposing the pdf distribution of the mean turbulent intensity coincident with a Gauss distribution, the standard deviation and the mean value, i.e. the most probable value, were derived. The aim was to compare the turbulent distribution for the four different geometries for comparing their performances around the ignition time: the more the mean turbulent intensity close to the spark plug, the more the combustion starting velocity. Furthermore the standard deviation parameter is key parameter for evaluating the engine inclination to the cyclic variability: the less the standard deviation, the less the cyclic variability tendency, because the more is the probability of having a value close to the most probable value in multiple consecutive engine cycles.
3. The tumble torque. The tumble torque (Fig. 2a) was measured across the intake valve during the suction phase. In particular, as depicted in Fig. 2b, the circumferential intake area of the valve was subdivided into four sections. The tumble torque TT was separately evaluated on each valve curtain sector by the following expression:

$$TT = \left[\left(\bar{b} \wedge \bar{v}\right) \times vers\_rot\right] \cdot \dot{m} \tag{1}$$

Where the term $\dot{m}$ is the intake mass flow rate, $\bar{b}$ is the distance between the inlet velocity vector $\bar{v}$ and the instantaneous piston center of gravity. The vector product of the vectors $\bar{b}$ and $\bar{v}$ is projected on the main tumble vortex axis, named *vers_rot*. The idea was to investigate the tumble formation measuring the tumble torque across the intake valve curtain area, which was subdivided into the four main sections: the liner side, the symplane side, the intake side, the exhaust side. The focus of this analysis was to highlight the different contribution of the tumble torque recorded in each sector on the whole tumble torque across the intake valve and therefore on the main in-cylinder structured tumble motion.

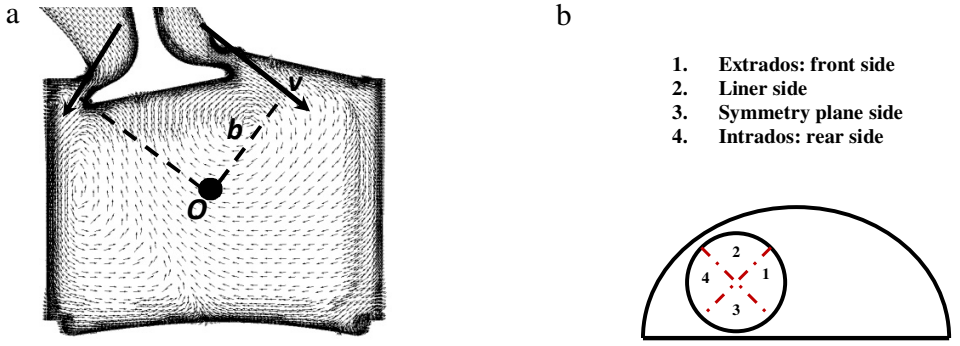

Fig. 2. (a) Tumble torque sketch; (b) Intake valve curtain area subdivision in four sectors.

4. The vortex type and number in the flow field. The authors studied the number of clockwise and counter-clockwise vortexes at IVC in the flow field. The idea is to explain the case in which the tumble ratio is high but the tumble breakdown is not so effective in generating the turbulence close to TDC. In fact the tumble ratio parameter is a mean value of the flow field: it could be high because the flow field is characterized or by one clockwise macro-vortex or by multiple vortexes, some clockwise and some counter-clockwise. In the last case the tumble breakdown is less effective than in the first case. A clockwise vortex is a vortex that gives a positive contribution to the tumble motion in the present reference system, while the counter-clockwise vortex has the opposite behavior. The vortex equation was derived under the hypothesis of free vortex:

$$\bar{V}_{tan} = \bar{\omega}_V \wedge \bar{r} \tag{2}$$

For each cell center of the mesh, located on the tumble plane, the free vortex equation was computed for a certain radius r. The tangential velocity V_{tan} of the vortex was derived by the CFD results and then the vortex angular velocity ω_i at the radius r was computed. If the vortex angular velocity has a value greater than a threshold value, there is a vortex centered in that cell center. For computing the threshold value, which represents a filter, the author supposed to consider a value which, divided for the engine rotational speed, gives a tumble ratio greater than the 75% of the tumble ratio at IVC by the CFD results. This is a hypothesis but it introduces a unique filter for comparing different results: the results obtained by the filtering operation are then comparable.

4.1. The tumble ratio and the mean turbulent intensity trends analysis

Fig. 3 and 4 show the in-cylinder tumble ratio and the mean turbulent intensity over the last simulated engine cycle period. The results are summed-up in Table 3 in terms of the maximum tumble ratio value, the tumble ratio value at IVC, the turbulent intensity value at IVC and its value at 700 deg. BTDC.

Table 3. Results from CFD analysis.

Case	Geometrical parameters	Maximum in-cylinder TR [-]	TR @ IVC [-]	u'/Vp @ IVC	u'/Vp @ 700 deg. BTDC
1	α=37, β=45	0.58	0.45	0.76	0.81
2	α=37, β=55	0.73	0.56	0.77	0.81
3	α=47, β=45	0.93	0.74	0.80	0.82
4	α=47, β=55	0.92	0.75	0.79	0.83

Starting from the tumble ratio evolutions, Fig. 3a show the tumble ratio trend from IVO to IVC for the four considered α/β combinations: the vortex generation phase (from IVO to BDC) and the vortex stabilization phase (from BDC to IVC) are clearly visible. Fig. 3b shows the same tumble ratio trend from IVC to TDC: the vortex spin-up phase (from IVC to 650 deg. BTDC) and the vortex breakdown phase (from 650 deg. BTDC to TDC) are well recognizable. In particular from Fig. 3a, it is possible to state that at 6500 rpm the Case 1 (α/β=37°/45°) was characterized by the lowest tumble ratio value at IVC. Starting from the Case 1, increasing the β angle from 45° to 55° (Case 2) the tumble ratio at IVC was increased of about the 24%. However, the maximum value for the tumble ratio at IVC was recorded increasing the α angle till its maximum value equal to 47°. Comparing the tumble ratio profiles obtained for the Case 1 and the Case 3 (Fig. 3), it is possible to verify as the increment of the α angle produced a tumble ratio increment at IVC of about the 64%. It clearly shows the quite different influence of the α and β angles on the in-cylinder tumble motion. It is underlined also by the tumble ratio trend obtained for the Case 4 (α/β=45°/55°) that was exactly the same of the Case 3: the further increase of the β angle from 45° to 55° when the α angle is at its maximum value did not produce any significant variation of the tumble ratio profile at 6500 rpm.

Fig. 4a shows that from IVC the mean turbulent intensity recorded for the Case 3 and Case 4 resulted the highest, showing the effectiveness of an increment of the α angle on the in-cylinder turbulence conditions. In Fig. 4 the probability distribution functions (pdf) of the turbulent intensity for all the examined cases were reported: they were recorded in the whole combustion chamber (Fig. 4b) and in a sphere having a radius of 1 cm and centered in the spark plug location (Fig. 4c). Comparing Fig. 4b and Fig. 4c the importance of a correct estimation of the turbulence level close to spark plug is evident: close to the ignition point the most probable value is higher than in the whole chamber and with a lower standard deviation. The pdf distribution close to the spark plug is almost the same for all the 4 geometries. A deep analysis of the pdf distribution of the turbulent intensity was carried out: it was supposed the pdf distribution coincident with a Gauss distribution, so the mean value, i.e. the most probable value, and the standard deviation were derived. In Fig. 5 the in-cylinder turbulent intensity mean values for all the geometries and the corresponding standard deviations were plotted. In Fig. 6 the turbulent intensity mean values close to the spark plug location and the corresponding standard deviations were plotted.

In Fig. 5a the maximum turbulent intensity value is for geometries having α equal to 47°. There is an evidence of the decrease of this value approaching the TDC position. The standard deviation value in the whole cylinder domain

is depicted in Fig. 5b: the less standard deviation is for the Case 1 of Table 2. It is well assessed that the combustion development is mainly dependent on the flow conditions close to the spark plug at the ignition time. In particular the mixture composition and the turbulence distribution are of importance.

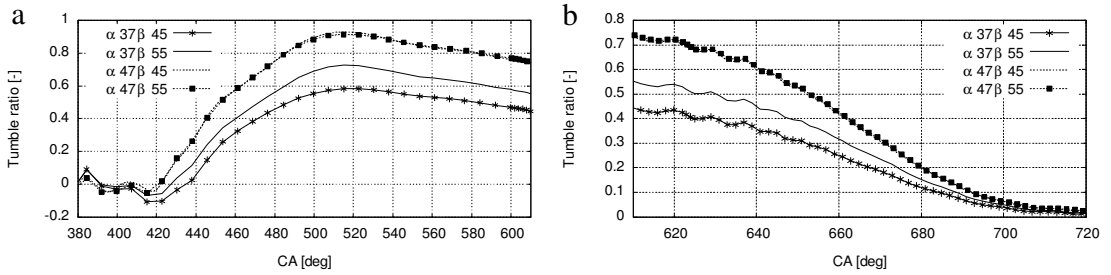

Fig. 3. (a) In-cylinder tumble ratio till IVC (610 deg. BTDC) ; (b) In-cylinder tumble ratio from till IVC to TDC.

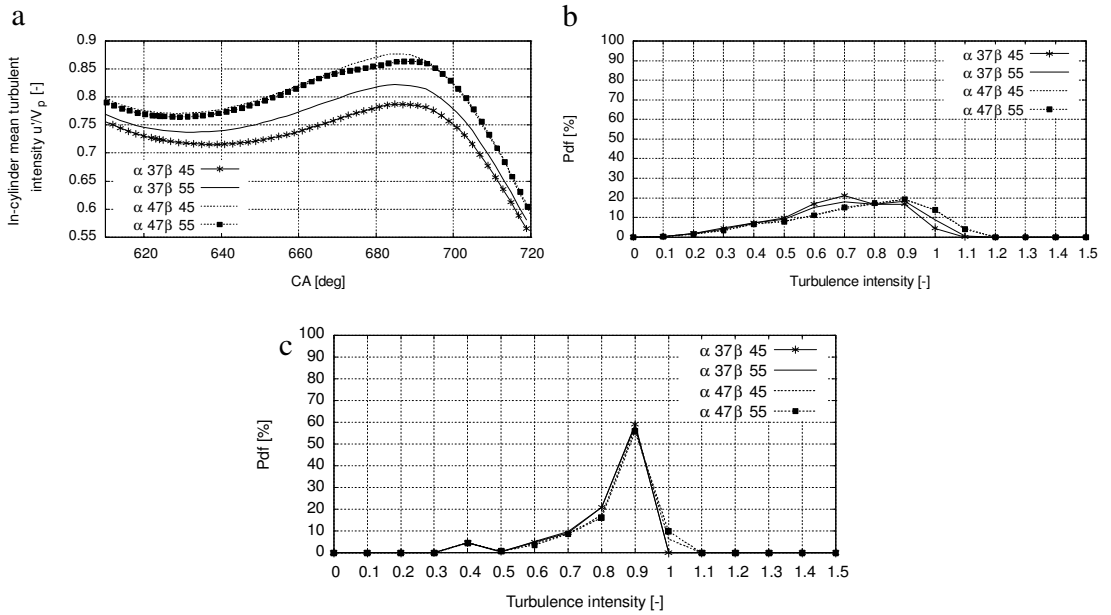

Fig. 4. (a) In-cylinder mean turbulent intensity u'/Vp; (b) In-cylinder mean turbulent intensity u'/Vp pdf trend at 700 deg. BTDC; (c) Close to spark plug (R 1cm) mean turbulent intensity u'/Vp pdf trend at 700 deg. BTDC.

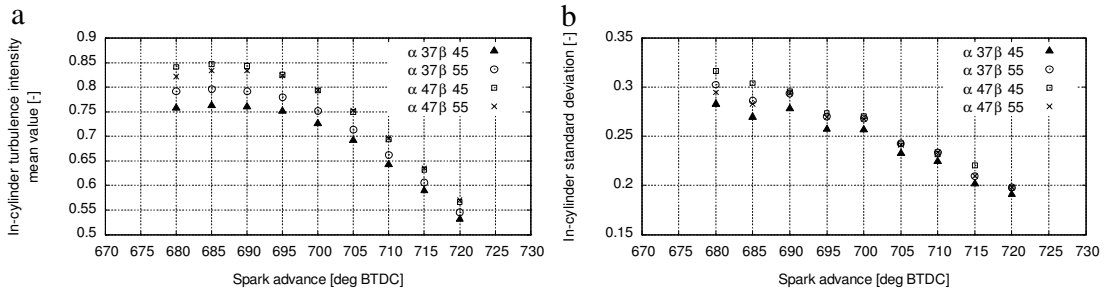

Fig. 5. (a) In-cylinder turbulent intensity u'/V_p mean value; (b) In-cylinder standard deviation of the turbulent intensity distribution.

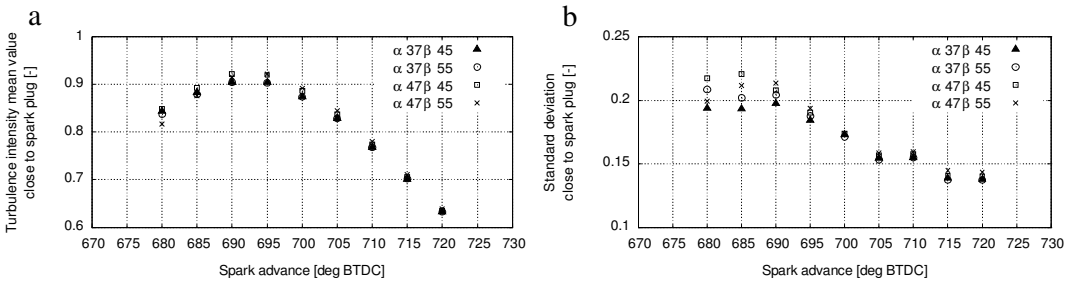

Fig. 6. (a) Turbulent intensity u'/V_p mean value close to spark plug; (b) Standard deviation of the turbulent intensity distribution close to spark plug.

It is to note the trend of the turbulent intensity close to spark plug in Fig. 6a: the value is almost constant in the range from 690 to 700 deg. BTDC and the maximum value is for the two geometries having the angle α equal to 47°. The standard deviation (Fig. 6b) seems to be almost independent from the geometry configuration starting from angle 700 deg. BTDC and it reaches its minimum value from 705 to 720 deg. BTDC. So the standard deviation is less if computed across the spark plug (Fig. 6b) than if measured in the whole domain: the less the standard deviation, the less the engine tendency to the cyclic variability. Anyway the best configuration appears to be the geometry α47β55, which has the highest turbulent intensity and the lowest standard deviation, especially in the range 695-700 deg. BTDC: this should be a suitable range of ignition for this kind of engine at 6500 rpm.

At this point the reasons of the better performances of the geometry α47β55 had to be explained: the authors introduced the tumble torque and the vortex analysis concepts.

4.2. The tumble torque analysis

In this paragraph an analytical analysis based on the tumble torque trend is carried out. In Fig. 7 the velocity vector profiles in the tumble plane across the intake valve were reported: looking at these pictures it is evident that it is difficult to graphically evaluate the tumble torque formation efficiency and moreover to compare them. So the authors decided to use the tumble torque parameter for an analytical comparison.

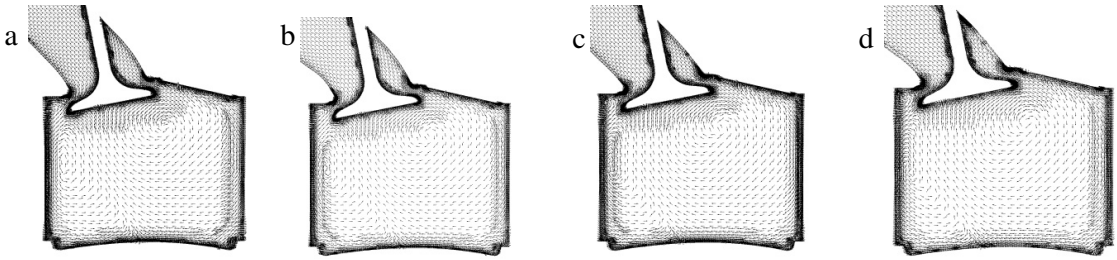

Fig. 7. Velocity vectors profile in the tumble plane across the intake valve at 540ca – Vectors range: 0÷120 m/s. (a) α=37 β=45; (b) α=37 β=55; (c) α=47 β=45; (d) α=47 β=55.

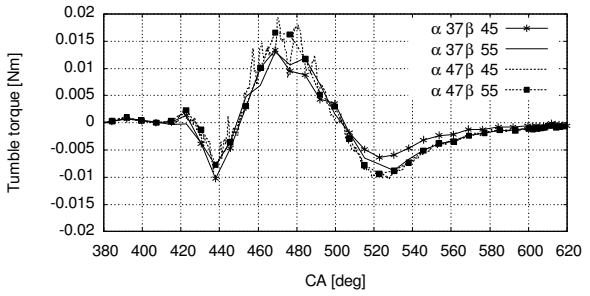

Fig. 8. Tumble torque trends for geometries summed up in Table 2.

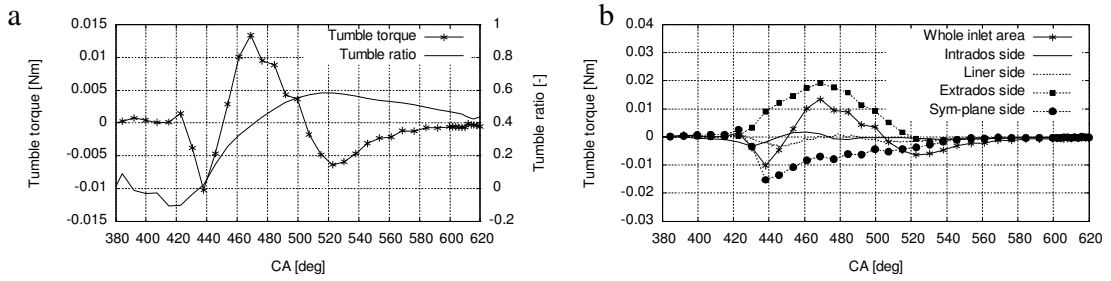

Fig. 9. Case 1 – α=37 β=45. (a) Comparison between tumble torque and tumble ratio till IVC; (b) Tumble torque across the intake valve split into the four main sectors.

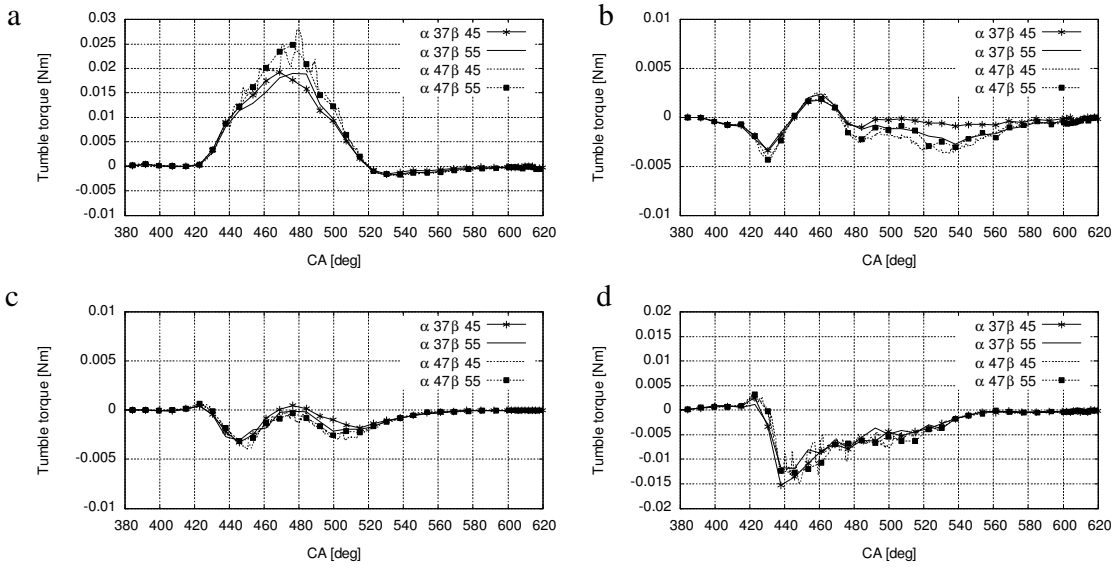

Fig. 10. Tumble torque trends. (a) Extrados side; (b) Intrados side; (c) Liner side; (d) Sym-plane side.

In Fig. 8 the tumble torque trends measured across the whole intake area for the 4 geometries of Table 2 were depicted: the tumble torque is higher for Cases 3 and 4, while is lower for Cases 1 and 2, confirming the results coming from the Fig. 3 (tumble ratio). Moreover the most important intake phase for the tumble torque is around the

maximum valve lift, i.e. 470 deg. BTDC, where the tumble torque is maximum. In Fig. 9, for example, the Case 1 (α37 – β45) is analyzed. In Fig. 9a the comparison between the tumble torque and the tumble ratio was plotted, while in Fig. 9b the tumble torque across the intake valve split in the four sectors was depicted. From the Fig. 9a it is to note that there is a strict relationship between the tumble torque and the tumble ratio: when the tumble torque is raising, there is a significant positive slope in the tumble ratio trend too, i.e. in the range between 440 and 500 deg. BTDC. In Fig. 9b the tumble torque in the extrados side is positive. The contribution of the tumble torque recorded in the liner side and in the intrados side is quite insignificant. The tumble torque recorded in the sym-plane side is negative, i.e. is counter-rotating: this causes an initial negative whole tumble torque because the tumble torque in the extrados side is lower than the tumble torque in the sym-plane side till the angle 450 deg. BTDC.

In Fig. 10 the results obtained splitting the whole intake area in four sectors were reported: in Fig. 10a the extrados side tumble torque trends for the four Cases in analysis were plotted. In Fig. 10b, 10c and 10d the intrados side tumble torque trend, the liner side tumble torque trend and the sym-plane side tumble torque trend were respectively depicted. Looking at Fig. 10 it is evident that the most important contribution derives from the extrados side and the sym-plane side of the intake duct, while the liner side (Fig. 10c) gives an almost null contribution to the tumble torque formation. In particular geometries α47β45 and α47β55 seem to have the maximum contribution to their tumble torque in the extrados side and the smallest one when the tumble torque is negative, i.e in the sym-plane side. These results confirm the findings above reported.

4.3. The vortex distribution analysis at IVC

In this paragraph an analysis of the vortexes of the flow field at IVC in each geometry configuration is presented. The aim was to investigate and to explain the difference in the flow field between the Case 3 and 4: they seem to have the same tumble motion and tumble torque, but the turbulent intensity distribution close to the spark plug is not exactly the same. The geometry α47β55 (Case 4) has a better tumble breakdown and so a better turbulent intensity distribution at the ignition start: this could strongly affect the combustion start and lower the cyclic variability of the engine. For understanding their difference in the flow field the authors studied the number of clockwise and counter-clockwise vortexes at IVC in both the two configurations.

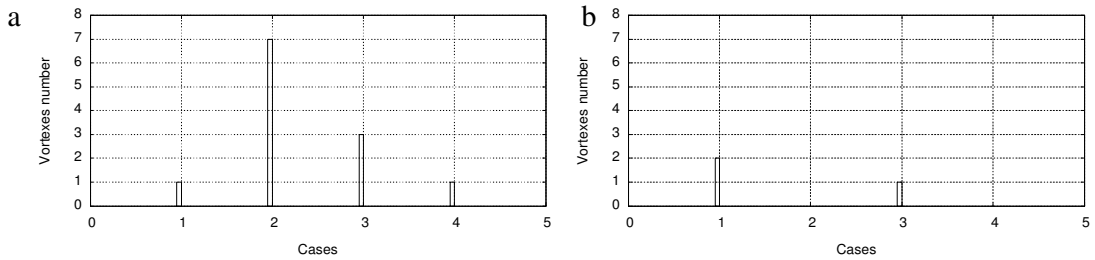

Fig. 11. (a) Clockwise rotating vortexes; (b) Counter-clockwise rotating vortexes.

The results of the vortex analysis are shown in Fig. 11: in Fig. 11a the number of clockwise vortexes for each geometry was plotted, while in Fig. 11b the counter-clockwise vortexes were reported. As visible, the Case 4 has one positive macro-vortex and no counter-clockwise vortexes, so it represents the best configuration. The Case 3 has three positive vortexes and two negative vortexes: this is the sign of a less structured flow field a IVC.

This methodology of analysis could give a help in the deep insight of the flow field structures generated during the intake phase. More details and pictures on the CFD results could be find in [4]: they were not reported here for brevity seeking.

5. Conclusions

In the current paper the results from the numerical CFD simulations performed to assess the influence of the intake duct geometrical parameters on the tumble motion generation during both the intake and the compression strokes were deeply analyzed.

In detail, the present analysis concerned the use of a methodological approach for studying the effect of the geometrical intake duct parameters not only on the tumble motion but also on the turbulence level. For this purpose the authors used the tumble torque analysis for understanding the process of the tumble formation during the intake phase. Then a deep insight of the turbulence generation was carried out: the pdf distribution of the turbulent intensity close to the spark plug position was reported. Assuming the pdf distribution coincident with the Gauss distribution, the standard deviation and the mean value (i.e. the most probable value) were derived for different angles close to TDC. These results seemed to suggest that the β angle has a less importance on the final distribution of the turbulence level around the spark plug at the ignition time: the last is relevant in determining the combustion start and then it influences the whole combustion process. Moreover the less the standard deviation, the less the engine tendency to the cyclic variability, keeping the detonation risk away. Nevertheless the geometry $\alpha 47 \beta 55$ showed to have the best breakdown, with a better distribution of the turbulent intensity close to the spark plug. A deep insight of the flow field was done by a new approach based on the analysis of the number and type of vortex in the combustion chamber at IVC.

In the next future, the proposed work will be completed by evaluating the influence on the in-cylinder turbulence conditions of the part-load condition.

References

[1] Falfari S, Bianchi GM, Nuti L. Numerical Comparative Analysis of In-Cylinder Tumble Flow Structures in Small PFI Engines Equipped by Heads Having Different Shapes and Squish Areas. ICES2012-81095. In: Proceedings of ASME Internal Combustion Engine Division, 2012. Spring Technical Conference.

[2] Falfari S, Brusiani F, Pelloni P. 3D CFD Analysis of the Influence of Some Geometrical Engine Parameters on Small PFI Engine Performances – The Effects on the Tumble Motion and the Mean Turbulent Intensity Distribution. ATI 2013 – 060-12178. ATI Congress 2013, Bologna. Italy. Accepted for publication on ATI 2013 Energy Procedia special issue.

[3] Falfari S, Bianchi GM, Nuti L. 3D CFD Analysis of the Influence of Some Geometrical Engine Parameters on Small PFI Engine Performances – The Effects on Tumble Motion and Mean Turbulent Intensity Distribution. SAE 2012-32-0096. SETC Congress, Madison, USA.

[4] Falfari S, Brusiani F, Bianchi GM. Assessment of the Influence of Intake Duct Geometrical Parameters on the Tumble Motion Generation in a Small Gasoline Engine. SAE 2012-32-0095. SETC Congress, Madison, USA.

[5] Falfari S, Brusiani F, Bianchi GM. Numerical Analysis of In-Cylinder Tumble Flow Structures – Parametric 0D Model Development. ATI 2013 – 060-12805. ATI Congress 2013, Bologna. Italy. Accepted for publication on ATI 2013 Energy Procedia special issue.

[6] Ramajo D, Zanotti A, Nigro N. Assessment of a zero-dimensional model of tumble in four-valve high performance engine. International Journal of Numerical Methods for Heat & Fluid Flow, Vol. 17 No. 8, 2007, pp. 770-787.

[7] Laget O, Zaccardi J.M, Gautrot X, Mansion T, Cotte E. Establishing New Correlations Between In-Cylinder Charge Motion and Combustion Process in Gasoline Engine Through a Numerical DOE. SAE paper 2010-01-0349.

[8] Church W, Farrell PV. Effects of Intake Port Geometry on Large Scale In-Cylinder Flows. SAE 980484.

[9] Miller R, Newman C, Dai W, Trigui N, Davis G, Trumpy D, Glidewell J. Up-Front Predictions of the Effects of Cylinder Head Design on Combustion Rates in SI Engines. SAE 981049.

[10] Arcoumanis, C, Godwin SN, Kim, JW. Effect of Tumble Strength on Combustion and Exhaust Emissions in a Single Cylinder, Four-Valve, Spark Ignition Engine. SAE 981044.

[11] Bianchi GM, Cantore G, Fontanesi S. Turbulence Modeling in CFD Simulation of ICE Intake Flows: The Discharge Coefficient Prediction. SAE TRANSACTIONS-SAE Journal of Engines, Vol. 111, Sect. 3, pp. 1901-1918, ISBN 0-7680-1287-2. Warrendale (PA, USA), 2003.

[12] Bianchi GM, Brusiani F, Grimaldi CN, Postrioti L, Carmignani L, Di Palma S, Marcacci M, Matteucci L. CFD Analysis of Injection Timing Influence on Mixture Preparation in a PFI Motorcycle Engine. SAE TRANSACTIONS-SAE Journal of Engines, Vol. 115, Sect. 3, pp.984-998, ISBN 978-0-7680-1835-6. Warrendale (PA, USA), 2007.

[13] Falfari S, Bianchi GM. Development of an Ignition Model for S.I. Engines Simulation. SAE Paper 2007-01-0148. In: SAE International Congress, Detroit, 2007.

[14] Bianchi GM, Brusiani F, Grimaldi CN, Postrioti L, Carmignani L, Marcacci M, Matteucci L. CFD Analysis of Injection Timing and Injector Geometry Influences on Mixture Preparation at Idle in a PFI Motorcycle Engine. SAE PAPER 2007-24-0041. In: SAE ICE2007 International Conference, 2007.

[15] Bianchi GM, Forte C, Corti C. Validation of a Lagrangian Ignition Model in SI Engine Simulations. ICEF2010-35159,. In: ASME – ICEF 2010, San Antonio, Texas, 2010.